Front. Energy 2020, 14(4): 882–888
https://doi.org/10.1007/s11708-020-0694-z

RESEARCH ARTICLE

Bin ZHAO, Xianze AO, Nuo CHEN, Qingdong XUAN, Mingke HU, Gang PEI

A spectrally selective surface structure for combined photothermic conversion and radiative sky cooling

Abstract The sun and outer space are the ultimate heat and cold sources for the earth, respectively. They have significant potential for renewable energy harvesting. In this paper, a spectrally selective surface structure that has a planar polydimethylsiloxane layer covering a solar absorber is conceptually proposed and optically designed for the combination of photothermic conversion (PT) and nighttime radiative sky cooling (RC). An optical simulation is conducted whose result shows that the designed surface structure (i.e., PT-RC surface structure) has a strong solar absorption coefficient of 0.92 and simultaneously emits as a mid-infrared spectral-selective emitter with an average emissivity of 0.84 within the atmospheric window. A thermal analysis prediction reveals that the designed PT-RC surface structure can be heated to 79.1°C higher than the ambient temperature in the daytime and passively cooled below the ambient temperature of approximately 10°C in the nighttime, indicating that the designed PT-RC surface structure has the potential for integrated PT conversion and nighttime RC utilization.

Keywords solar energy, photothermic conversion, radiative sky cooling, spectral selectivity, multilayer film

1 Introduction

The practice of harvesting heat and coolness for buildings from renewable energy sources has recently been a hot topic in energy fields. Photothermic conversion (PT) is one such method to provide heat for buildings and there are already numerous kinds of commercial PT products for energy saving of buildings, such as the flat-plate solar collector [1], the evacuated tube collector [2], and the trombe wall [3]. Recently, radiative sky cooling (RC) has been widely investigated as an alternative cooling method to provide cooling and/or dissipate heat passively, and, it has successfully applied in many potential applications such as building-scale cooling supply [4], radiative cooling of solar cells [5,6], personal thermal management [7], and power generation [8].

The principle of RC is that heat is radiated from the surface to the cold outer space in the form of electromagnetic waves, relying on the transparent "atmospheric window" to allow thermal emission within the wavelength range of 8 to 13 μm to effectively escape to the universe [9,10]. Early work on RC focused on cooling passively at night. Materials that have a high emissivity within the atmospheric window are good candidates of emitter for efficient nighttime RC [11], such as commercial black paint [12,13], silicon monoxide films [14,15], and tedlar film [16]. On the building system level, RC can be integrated into buildings for cooling supply. For example, Parker and Sherwin [17] developed a NightCool building that integrates an RC emitter as the roof. A long-term experiment test was conducted and the results showed that the average energy saving of this building can reach 15%. More recently, the concept of self-cooling below the ambient temperature by the RC method in the daytime has also been demonstrated and aroused a lot of interests. Numerous advanced RC emitters, including photonic structures [9,18], metamaterials [19,20], and other novel materials [21,22] have been developed and investigated. For example, Raman et al. [9] developed a multilayer emitter that can reflect approximately 97% incident solar radiation and emits strongly only within the atmospheric window. Nearly 5°C below the ambient temperature and a cooling power of 40.1 W/m^2 were experimentally achieved

Received Feb. 15, 2020; accepted May 15, 2020; online Sept. 15, 2020

Bin ZHAO, Xianze AO, Nuo CHEN, Qingdong XUAN, Gang PEI (✉)
Department of Thermal Science and Energy Engineering, University of Science and Technology of China, Hefei 230027, China
E-mail: peigang@ustc.edu.cn

Mingke HU (✉)
Department of Thermal Science and Energy Engineering, University of Science and Technology of China, Hefei 230027, China; Institute of Sustainable Energy Technology, University of Nottingham, University Park, Nottingham NG7 2RD, UK
E-mail: Mingke.Hu@nottingham.ac.uk

by this emitter. However, although daytime RC has been demonstrated, the solar reflection requirement of the emitter is too trenchant since solar radiation power is nearly a magnitude higher than the net RC cooling power. Thus, compared with daytime RC, nighttime RC is easier for implementation.

Based on the spectral response of the PT absorber and RC emitter to the electromagnetic waves, a concept was previously proposed to achieve solar thermal collection by PT at daytime and cooling by RC at night using a spectrally selective surface structure, which makes the system work all day by the two different functions. This concept is named PT-RC hybrid utilization and the spectrally selective surface that achieves these two functions is called a PT-RC surface structure. The PT-RC surface structure needs to have a high solar absorption and strong thermal emission only within the atmospheric window. This idea of PT-RC hybrid utilization was presented previously [23,24] where a kind of PT-RC surface structure that consists of a titanium-based absorber and a polyethylene terephthalate film (TPET) was manufactured. This paper further contributes to the PT-RC hybrid utilization principle by designing a new kind of spectrally selective PT-RC surface structure. Specifically, a broadband spectral response optimization of the PT-RC surface structure is performed, which updates the design methods of the PT-RC surface structure from the optical design perspective. Notably, this method can be extended to be a general guide for the design of spectral selective coating in other fields, such as the solar absorber and optical filters.

In this paper, a new PT-RC surface structure for the integration of daytime PT and nighttime RC is designed by covering a solar absorber with a planar polydimethylsiloxane (PDMS) film. Besides, an optical simulation is conducted to evaluate the spectral properties of this PT-RC surface structure. Moreover, a thermal analysis based on a steady-state heat transfer process is applied to investigate the thermal performance of the designed PT-RC surface structure. Furthermore, the performance of the designed and the ideal PT-RC surface structure is compared.

2 Optical design of PT-RC surface structure

The schematic of the PT-RC hybrid utilization is illustrated in Fig. 1(a). For an optimal combination of daytime PT and nighttime RC, the PT-RC surface structure needs to satisfy the following spectral requirements as shown in Fig. 1(b). First, the PT-RC surface structure needs to have a high solar absorption to maximally harvest solar energy. Next, the PT-RC surface structure needs to exhibit a strong thermal emission within the atmospheric window to generate a sub-ambient cooling environment at nighttime. Finally, the PT-RC surface structure needs to have a low absorptivity/emissivity within the remaining wavelength band (i.e., 3–8 μm and > 13 μm) to reduce the heat and cooling loss during combination.

The schematic of the designed PT-RC surface structure is depicted in Fig. 2(a). The PT-RC surface structure consists of three layers that are fixed on a reflective

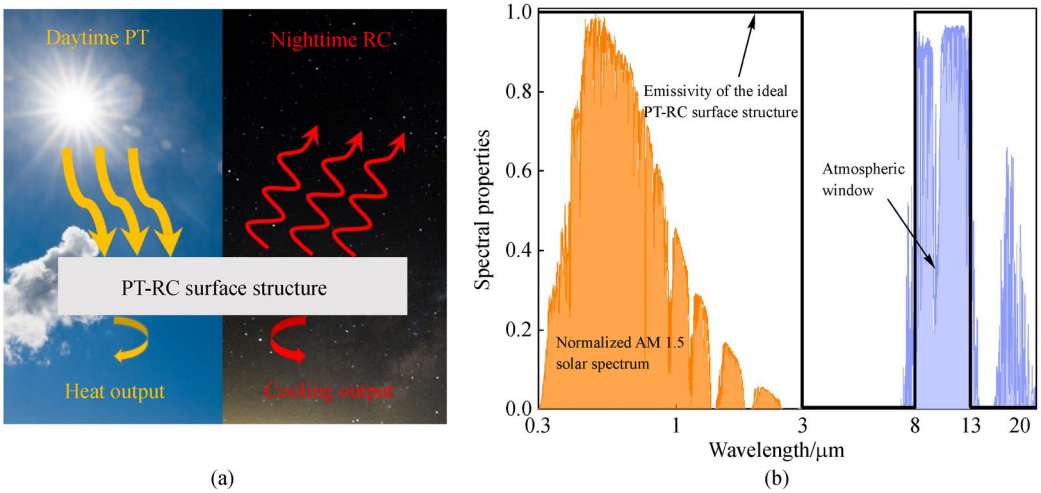

Fig. 1 Schematic of PT-RC hybrid utilization and spectral requirement of the ideal PT-RC surface structure.
(a) Schematic of PT-RC hybrid utilization; (b) emissivity/absorptivity spectra of ideal PT-RC surface structure, with normalized AM 1.5 solar spectrum[1)] and a transmittance curve of atmospheric window[2)] presented as references.

1) Reference solar spectral irradiance: ASTM G-173. 2019–12–12, available at website of rredc.nrel.gov
2) MODTRAN infrared light in the atmosphere. 2019–12–12, available at website of climatemodels.uchicago.edu

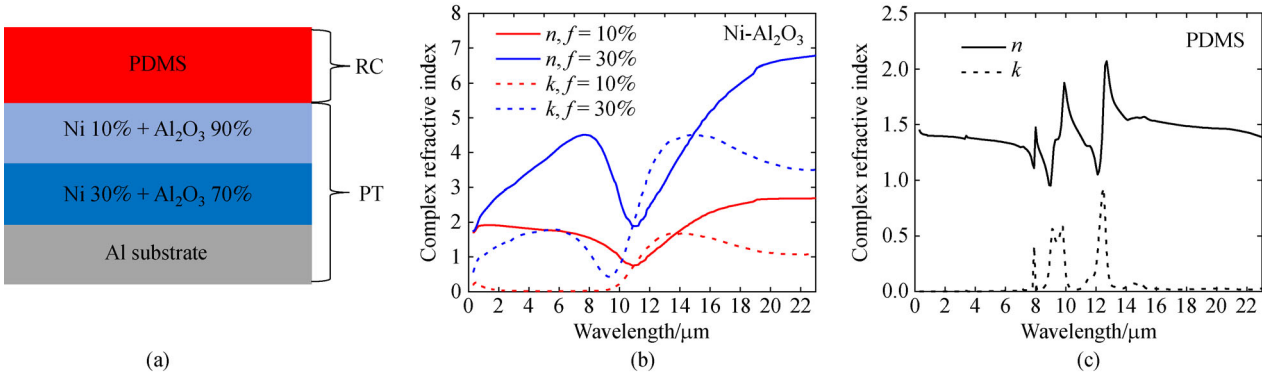

Fig. 2 Schematic of the proposed PT-RC surface structure and complex refractive index of related material.
(a) Schematic of PT-RC surface structure; (b) and (c) complex refractive index of Ni-Al_2O_3 mixing material and PDMS material.

aluminum (Al) substrate. The spectral response of the proposed PT-RC surface structure is optically simulated and optimized using TFCalc™ software (version 3.5) [25]. During optimization, the program varies the thickness of the layers to minimize the evaluation merit function as expressed in Eq. (1).

$$F = \left(\frac{1}{m} \sum_{j=1}^{m} \left| \frac{I_j D_j C_j - T_j}{N_j (\mathrm{Tol})_j} \right|^p \right)^{1/p}, \quad (1)$$

where F is the value of merit function, I denotes the intensity of the illuminant, D denotes the efficiency of the detector, C and T are the simulated and target value, N and Tol represent the normalized factor and tolerance for the target, p is the power of the method, m is the number of the target, and j means target j. The target of this design is the spectral emissivity of the multilayer film and the target value is set to be the emissivity value of the ideal PT-RC surface structure, as shown in Fig. 1(b).

During the optical simulation, the spectral-dependent complex refractive indexes that include the refractive index (n) and extinction coefficient (k) of Al, nickel (Ni), aluminum oxide (Al_2O_3), and PDMS are extracted from Refs. [26–29]. The effective optical constant of the mixing layer of Ni-Al_2O_3 is determined by using the Bruggeman model [30,31]

$$f \frac{\xi_{\mathrm{Ni}} - \xi_{\mathrm{Ni\text{-}Al_2O_3}}}{\xi_{\mathrm{Ni}} + 2\xi_{\mathrm{Ni\text{-}Al_2O_3}}} + (1-f) \frac{\xi_{\mathrm{Al_2O_3}} - \xi_{\mathrm{Ni\text{-}Al_2O_3}}}{\xi_{\mathrm{Al_2O_3}} + 2\xi_{\mathrm{Ni\text{-}Al_2O_3}}} = 0, \quad (2)$$

where ξ denotes the complex permittivity and f represents the volume fraction of Ni in the Ni-Al_2O_3 mixing layer. The complex refractive indexes of Ni-Al_2O_3 mixing material (f = 10% and 30%) and PDMS material are presented in Figs. 2(b) and 2(c) for references.

The optimized spectral response of the designed PT-RC surface structure is demonstrated in Fig. 3 and the corresponding thickness of each layer is given in Table 1. For the normal incident condition, the designed PT-RC surface structure has a high solar absorption with a weighted absorptivity of nearly 0.92 and emits strongly and selectively within the atmospheric window with an energy-averaged emissivity of 0.84 at the temperature of

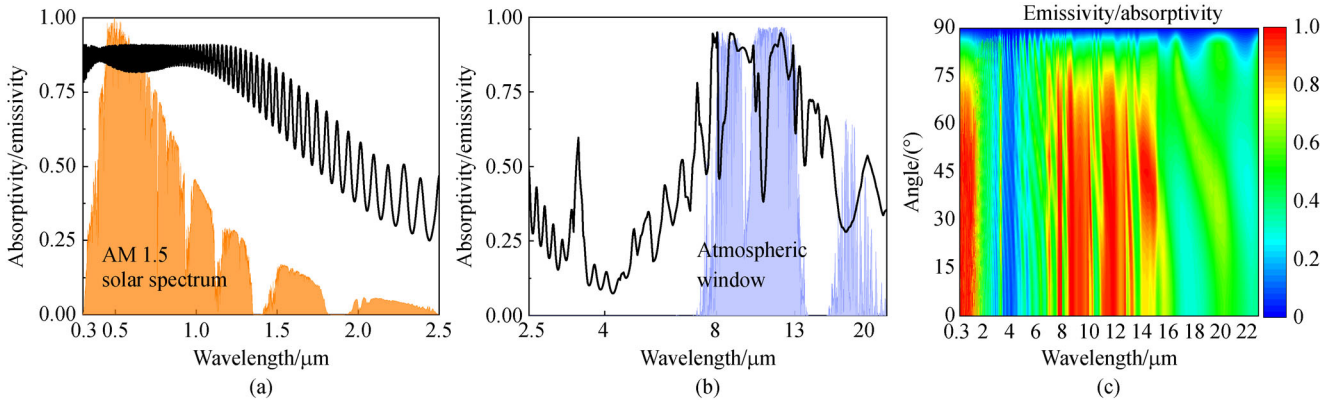

Fig. 3 Optimized spectral response of the designed PT-RC surface structure.
(a) Spectral absorptivity of designed PT-RC surface structure in solar radiation band; (b) spectral emissivity of designed PT-RC surface structure in mid-infrared wavelength band; (c) angle-dependent emissivity of designed PT-RC surface structure.

Table 1 Thickness of each layer of the designed PT-RC surface structure

Layer material	Thickness/nm
PDMS	18227
Ni 10% + Al_2O_3 90% (f = 10%)	75
Ni 30% + Al_2O_3 70% (f = 30%)	84

300 K. To investigate the sensitivity of the incident angle on the spectral response of the designed structure, the incident angle-dependent emissivity is calculated and presented in Fig. 3(c). It is found that the spectral response of the designed PT-RC surface structure remains similar when the incident angle is below approximately 70°, which is a good feature for the real application. Furthermore, the sensitivity of the PDMS layer thickness on the spectral response of the designed PT-RC surface structure is investigated. During the calculation process, the PDMS layer thickness is set as 18100 nm, 18200 nm, and 18300 nm, respectively. As shown in Fig. 4, the spectral response curves under these layer thicknesses are almost the same, indicating that the spectral response of the designed PT-RC surface structure is not sensitive to this parameter when the PDMS layer thickness changes within a small range.

In this PT-RC surface structure, the bottom two layers with the Al substrate are responsible for solar collection, which is a typical kind of solar absorber known as the nickel-aluminum oxide (Ni-Al_2O_3) coating [32]. The PDMS layer primarily assists in optimizing the spectrally selective thermal emission in the mid-infrared wavelength band. The PDMS film has a high solar transmittance and emits strongly within the atmospheric window so that the solar radiation can be harvested by Ni-Al_2O_3 solar absorber and the waste heat can be radiated away. In addition, the PDMS material is typically used as a solar transparent emitter for efficient RC applications [33,34].

3 Thermal analysis

To evaluate the thermal performance of the designed PT-RC surface structure, the heat balance equation of the surface structure is numerically solved to calculate the stagnation temperature of the PT-RC surface structure in a 24-h timeframe. As displayed in Fig. 5, the PT-RC surface structure absorbs solar radiation P_{sun} and atmospheric radiation P_{atm}, and it radiates thermal emission P_{rad}. Moreover, the heat transfer process between the PT-RC surface structure and ambient air occurs by non-radiative methods (i.e., conduction and convection) and is depicted as $P_{\text{non-rad}}$ in Fig. 5. In the simulation, the temperature of the PT-RC surface structure is assumed to be uniform since the PT-RC surface structure is very thin and the components are thermally conductive materials. Besides, the PT-RC surface structure is placed horizontally.

Thermodynamically, the control equation of the PT-RC surface structure is expressed as

$$\frac{cm}{A}\frac{\partial T}{\partial t} = \sum P, \tag{3}$$

where c, m, A, and T are heat capacity, mass, area, and temperature of the PT-RC surface structure, respectively; t denotes time; $\sum P$ is net energy power into the surface structure. Here, a steady-state condition is assumed for PT-RC surface structure, which has already been used for preliminary performance prediction for RC and solar collection in Refs. [9,22,35]. Therefore, Eq. (3) can be presented as

$$P_{\text{rad}} - (P_{\text{atm}} + P_{\text{sun}} + P_{\text{non-rad}}) = 0. \tag{4}$$

In Eq. (4), $P_{\text{rad}} = 2\pi \int_0^{\infty} \int_0^{\frac{\pi}{2}} \varepsilon(\lambda,\theta) I_{\text{BB}}(\lambda,T) \sin\theta \cos\theta \, \mathrm{d}\theta \, \mathrm{d}\lambda$ is the thermal emissive power of the surface structure, where $\varepsilon(\lambda,\theta)$ denotes the directional spectral emissivity of

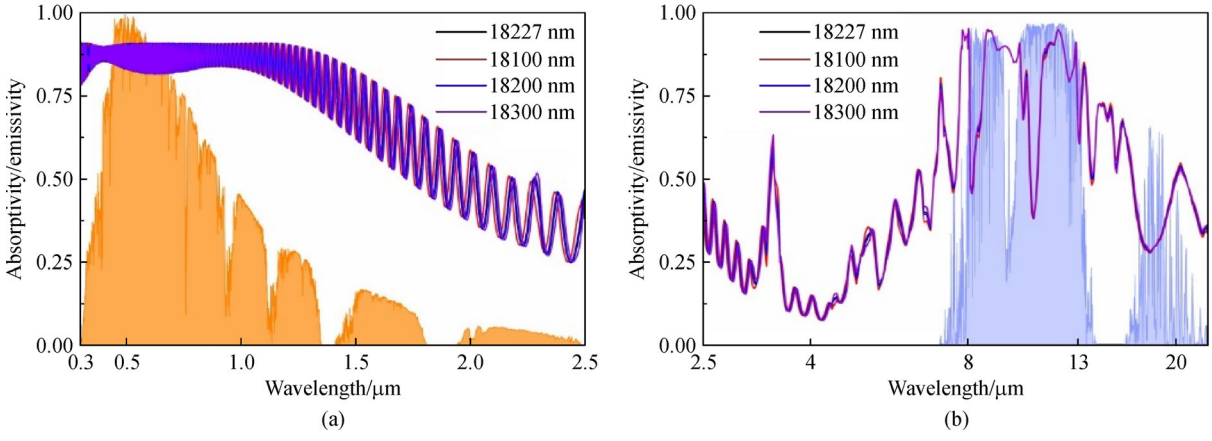

Fig. 4 Spectral absorptivity/emissivity of designed PT-RC surface structure with different PDMS layer thicknesses. (a) Solar radiation band; (b) mid-infrared wavelength band.

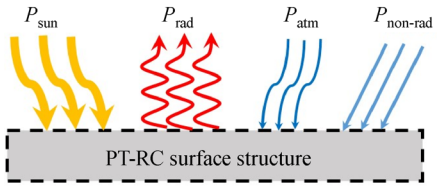

Fig. 5 Schematic of the heat transfer process of the PT-RC surface structure.

the surface structure; $I_{BB}(\lambda,T)$ is the spectral radiance of a blackbody at temperature T; $P_{atm} = 2\pi\int_0^{\infty}\int_0^{\frac{\pi}{2}}\alpha(\lambda,\theta)\varepsilon_{atm}(\lambda,\theta)I_{BB}(\lambda,T_{amb})\sin\theta\cos\theta d\theta d\lambda$ is the absorbed atmospheric radiation power, where $\alpha(\lambda,\theta)$ is the directional spectral absorptivity of the PT-RC surface structure; $\varepsilon_{atm}(\lambda,\theta)$ is the directional spectral emissivity of the atmosphere and it can be evaluated as $\varepsilon_{atm}(\lambda,\theta) = 1-\tau(\lambda,0)^{1/\cos\theta}$, where $\tau(\lambda,0)$ is the transmittance of the atmosphere at the normal direction; and T_{amb} is ambient temperature; $P_{sun} = \alpha_{total}G_s$ is the absorbed solar radiation power, where α_{total} is the total solar absorption of the PT-RC surface structure, which is weighted by the standard AM1.5 solar spectrum. G_s denotes the received solar power; $P_{non\text{-}rad} = h_{non\text{-}rad}(T_{amb}-T)$ is the heat power obtained from the environment by parasitic convection and conduction, where $h_{non\text{-}rad}$ is the overall heat transfer coefficient between the structure and the environment, which contains the effects of numerous parameters, such as wind speed and insulation condition of the PT-RC surface structure.

The equilibrium temperature of the PT-RC surface structure is predicted in a 24-h circle whose result is exhibited in Fig. 6. The solar radiation power and ambient temperature data used in the prediction process were experimentally measured at Hefei, China on April 16, 2018. The normal transmittance of the atmosphere under a clear sky condition is used and the data are obtained from the website[1)]. Furthermore, the overall heat transfer coefficient is set to be 5 W/(m^2·K) for preliminary analysis and this kind of assumption is used in mathematical prediction in Refs. [36,37].

Figure 6 indicates that the PT-RC surface structure is dramatically heated up by increased solar radiation power in the daytime. For example, the temperature of the PT-RC surface structure ($T_{PT\text{-}RC}$) reaches 102.2°C when the solar radiation power is 962.7 W/m^2, which is 79.1°C higher than the ambient air temperature, indicating that the designed surface structure can be potentially used to harvest solar radiation and transfer it into heat. At night, the PT-RC surface structure is passively cooled below the ambient air temperature due to its high thermal emissivity within the atmospheric window. The average temperature reduction of the PT-RC surface structure is approximately 10°C.

To compare the performance of the designed PT-RC surface structure with the ideal PT-RC surface structure (ideal spectral property is shown in Fig. 1(b)) and blackbody surface, the surface equilibrium temperatures under different solar radiation power conditions in the daytime and the net cooling power of the surface under different surface temperature conditions at night are evaluated. In comparison, the ambient temperature and overall heat transfer coefficient are set as 30°C and 5 W/(m^2·K), respectively. As shown in Fig. 7(a), the equilibrium temperature of the designed PT-RC surface structure is lower than that of the ideal PT-RC surface structure but greater than that of the blackbody surface even though the solar absorption of the designed PT-RC

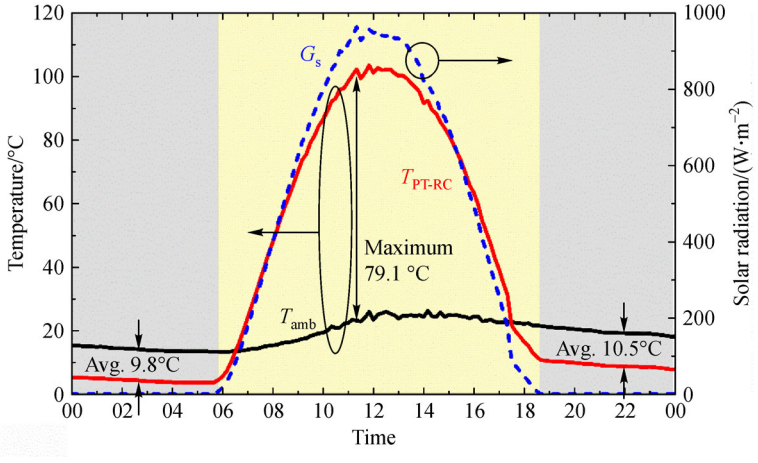

Fig. 6 Predicted temperature of PT-RC surface structure (red curve) at a 24-h circle, with ambient temperature (black curve) and solar radiation power (blue curve), plotted as references.

1) MODTRAN infrared light in the atmosphere. 2019–12–12, available at website of climatemodels.uchicago.edu

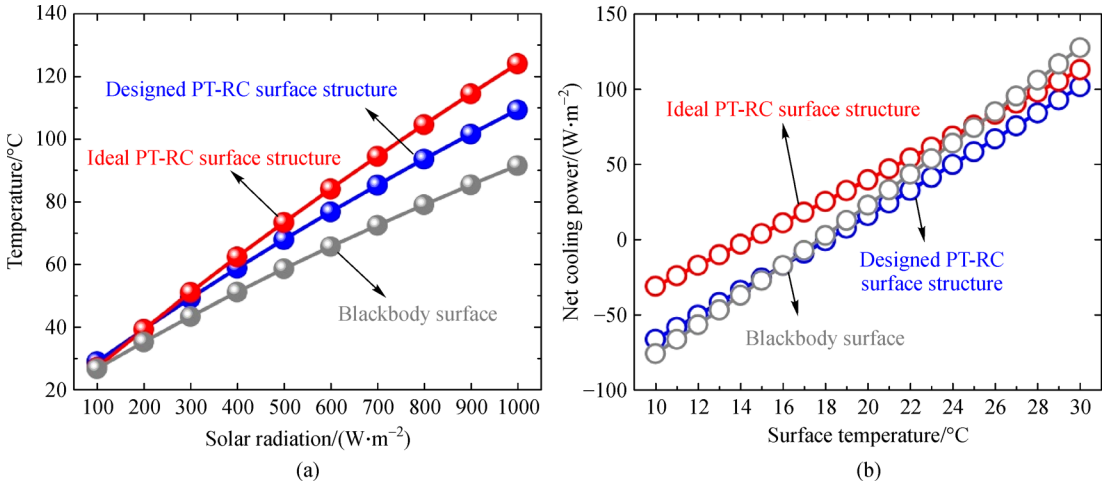

Fig. 7 Performance comparison of designed PT-RC surface structure, ideal PT-RC surface structure, and blackbody surface. (a) Equilibrium temperature of surface under different solar radiation power conditions in the daytime; (b) net cooling power of surface under different surface temperature conditions at night.

surface structure is approximately 8% lower than that of the blackbody surface. Besides, the temperature difference between the designed PT-RC surface structure and ideal PT-RC surface structure as well as between the designed PT-RC surface structure and blackbody surface both enlarge with increasing solar radiation power. As for the capacity of nighttime RC, Fig. 7(b) shows the net cooling power of three surfaces. Obviously, the minimum temperature of the ideal PT-RC surface structure is lower than that of the blackbody surface and the maximum net cooling power of the former is also inferior to the latter. This property is a typical characteristic between spectrally selective RC emitter (i.e., the ideal PT-RC surface structure) and blackbody emitter (i.e., blackbody surface). Furthermore, it is found that the cooling performance of the designed PT-RC surface structure is between the ideal PT-RC surface structure and blackbody surface. When the surface temperature is low, the cooling power of the designed PT-RC surface structure is close to that of the blackbody surface. However, when the surface temperature increases, the cooling power of the designed PT-RC surface structure behaves like the ideal PT-RC surface structure. The reason for this is that the spectral selectivity of the designed PT-RC coating is limited and atmospheric radiation outside of the atmospheric window is absorbed by the designed PT-RC surface structure.

4 Conclusions

In summary, a multilayer surface structure (i.e., PT-RC surface structure) is optically designed by covering a solar absorber with a PDMS film for hybrid utilization of PT and nighttime RC. Besides, a combined optical and thermal simulation is conducted to investigate the performance of the designed PT-RC surface structure. Based on the findings, the following conclusions can be reached.

The spectral selectivity of the deigned PT-RC surface structure is obvious. The PT-RC surface structure has a high solar absorption with an effective value of approximately 0.92 and simultaneously emits selectively within the mid-infrared wavelength band with an average emissivity of 0.84 in the atmospheric window, and it has a low emissivity in the remaining wavelength band.

The designed PT-RC surface structure is feasible for hybrid utilization of PT and RC. The surface structure can be heated to 79.1°C higher than the ambient air temperature in the daytime and can be passively cooled to approximately 10°C below the ambient air temperature at night.

Acknowledgements This work was supported by the National Natural Science Foundation of China (Grant Nos. 51776193, 51761145109, and 51906241).

References

1. Gang P, Huide F, Huijuan Z, Jie J. Performance study and parametric analysis of a novel heat pipe PV/T system. Energy, 2012, 37(1): 384–395
2. Sabiha M A, Saidur R, Mekhilef S, Mahian O. Progress and latest developments of evacuated tube solar collectors. Renewable & Sustainable Energy Reviews, 2015, 51: 1038–1054
3. Hu Z, He W, Ji J, Zhang S. A review on the application of Trombe wall system in buildings. Renewable & Sustainable Energy Reviews, 2017, 70: 976–987
4. Lu X, Xu P, Wang H, Yang T, Hou J. Cooling potential and applications prospects of passive radiative cooling in buildings: the current state-of-the-art. Renewable & Sustainable Energy Reviews, 2016, 65: 1079–1097

5. Zhao B, Hu M, Ao X, Xuan Q, Pei G. Spectrally selective approaches for passive cooling of solar cells: a review. Applied Energy, 2020, 262: 114548
6. Zhu L, Raman A, Wang K X, Anoma M A, Fan S. Radiative cooling of solar cells. Optica, 2014, 1(1): 32–38
7. Hsu P C, Song A Y, Catrysse P B, Liu C, Peng Y, Xie J, Fan S, Cui Y. Radiative human body cooling by nanoporous polyethylene textile. Science, 2016, 353(6303): 1019–1023
8. Raman A P, Li W, Fan S. Generating light from darkness. Joule, 2019, 3(11): 2679–2686
9. Raman A P, Anoma M A, Zhu L, Rephaeli E, Fan S. Passive radiative cooling below ambient air temperature under direct sunlight. Nature, 2014, 515(7528): 540–544
10. Zhao B, Hu M, Ao X, Chen N, Pei G. Radiative cooling: a review of fundamentals, materials, applications, and prospects. Applied Energy, 2019, 236: 489–513
11. Granqvist C G. Radiative heating and cooling with spectrally selective surfaces. Applied Optics, 1981, 20(15): 2606–2615
12. Ito S, Miura N. Studies of radiative cooling systems for storing thermal energy. ASME Journal of Solar Energy Engineering, 1989, 111(3): 251–256
13. Hu M, Zhao B, Ao X, Feng J, Cao J, Su Y, Pei G. Experimental study on a hybrid photo-thermal and radiative cooling collector using black acrylic paint as the panel coating. Renewable Energy, 2019, 139: 1217–1226
14. Granqvist C G, Hjortsberg A. Radiative cooling to low temperatures: general considerations and application to selectively emitting SiO films. Journal of Applied Physics, 1981, 52(6): 4205–4220
15. Granqvist C G, Hjortsberg A. Surfaces for radiative cooling: silicon monoxide films on aluminum. Applied Physics Letters, 1980, 36(2): 139–141
16. Catalanotti S, Cuomo V, Piro G, Ruggi D, Silvestrini V, Troise G. The radiative cooling of selective surfaces. Solar Energy, 1975, 17 (2): 83–89
17. Parker D S, Sherwin J R. Evaluation of the night cool nocturnal radiation cooling concept : annual performance assessment in scale test buildings. Program Report. 2008
18. Rephaeli E, Raman A, Fan S. Ultrabroadband photonic structures to achieve high-performance daytime radiative cooling. Nano Letters, 2013, 13(4): 1457–1461
19. Zhai Y, Ma Y, David S N, Zhao D, Lou R, Tan G, Yang R, Yin X. Scalable-manufactured randomized glass-polymer hybrid metamaterial for daytime radiative cooling. Science, 2017, 355(6329): 1062–1066
20. Fan S, Raman A. Metamaterials for radiative sky cooling. National Science Review, 2018, 5(2): 132–133
21. Mandal J, Fu Y, Overvig A C, Jia M, Sun K, Shi N N, Zhou H, Xiao X, Yu N, Yang Y. Hierarchically porous polymer coatings for highly efficient passive daytime radiative cooling. Science, 2018, 362 (6412): 315–319
22. Li T, Zhai Y, He S, Gan W, Wei Z, Heidarinejad M, Dalgo D, Mi R, Zhao X, Song J, Dai J, Chen C, Aili A, Vellore A, Martini A, Yang R, Srebric J, Yin X, Hu L. A radiative cooling structural material. Science, 2019, 364(6442): 760–763
23. Hu M, Pei G, Li L, Zheng R, Li J, Ji J. Theoretical and experimental study of spectral selectivity surface for both solar heating and radiative cooling. International Journal of Photoenergy, 2015, 2015: 1–9
24. Hu M, Pei G, Wang Q, Li J, Wang Y, Ji J. Field test and preliminary analysis of a combined diurnal solar heating and nocturnal radiative cooling system. Applied Energy, 2016, 179: 899–908
25. TFCalc. Version 3.5. Portland: Software Spectra, 2019
26. Querry M.Optical constants of minerals and other materials from the millimeter to the ultraviolet. Contract Report, 1987
27. Gupta V, Probst P T, Goßler F R, Steiner A M, Schubert J, Brasse Y, König T A F, Fery A. Mechanotunable surface lattice resonances in the visible optical range by soft lithography templates and directed self-assembly. ACS Applied Materials & Interfaces, 2019, 11(31): 28189–28196
28. Palik E D. Handbook of Optical Constants of Solids. San Diego: Elsevier, 1985
29. Refractive Index. 2019–5–24, available at website of refractiveindex.info
30. Niklasson G A, Granqvist C G, Hunderi O. Effective medium models for the optical properties of inhomogeneous materials. Applied Optics, 1981, 20(1): 26–30
31. Chester D, Bermel P, Joannopoulos J D, Soljacic M, Celanovic I. Design and global optimization of high-efficiency solar thermal systems with tungsten cermets. Optics Express, 2011, 19(S3): A245–A257
32. Li Z, Zhao J, Ren L. Aqueous solution-chemical derived Ni-Al_2O_3 solar selective absorbing coatings. Solar Energy Materials and Solar Cells, 2012, 105: 90–95
33. Kou J L, Jurado Z, Chen Z, Fan S H, Minnich A J. Daytime radiative cooling using near-black infrared emitters. ACS Photonics, 2017, 4 (3): 626–630
34. Lee E, Luo T. Black body-like radiative cooling for flexible thin-film solar cells. Solar Energy Materials and Solar Cells, 2019, 194: 222–228
35. Zhao B, Hu M, Ao X, Chen N, Xuan Q, Jiao D, Pei G. Performance analysis of a hybrid system combining photovoltaic and nighttime radiative cooling. Applied Energy, 2019, 252: 113432
36. Bao H, Yan C, Wang B, Fang X, Zhao C Y, Ruan X. Double-layer nanoparticle-based coatings for efficient terrestrial radiative cooling. Solar Energy Materials and Solar Cells, 2017, 168: 78–84
37. Ono M, Chen K, Li W, Fan S. Self-adaptive radiative cooling based on phase change materials. Optics Express, 2018, 26(18): A777–A787